Magyar Állami Eötvös Loránd Geofizikai Intézet
GEOFIZIKAI KÖZLEMÉNYEK
XX. kötet, 3–4. szám

AN ANALYSIS OF THE INITIAL SEISMIC PULSE NEAR UNDERGROUND EXPLOSIONS

T. BODOKY–G. KORVIN–I. LIPTAI–J. SIPOS*

The experiments were carried out in 1968 and 1969, in the Nyir-region, Hungary, in a nearsurface sandy complex characteristic of this area. The primary aim of the investigations was to determine the basic characteristics of the seismic pulse, its dependence on depth and charge weight, further its change during propagation. A detailed knowledge of these parameters has been rendered necessary by digital seismic data processing, where a realistic initial wave shape is indispensable for the deconvolution process.

The method and instrument of experiment

A barium-titanate crystal was used as detector, for the measurements. The unit-amplification matching member was mounted in a water-proof sonde-case holding the crystal. Signals from the crystal passed through this member to the recorder. The latter was a storage-system Textronix oscilloscope provided with a photo-adapter.

The main data of the sensing head: material: $BaTiO_3$ ceramics; diameter 20 mm; natural frequency 500 kcps; measuring range 0,1–100,0 atm; capacity 1670 pF; sensitivity 230 mV/atm; attenuating block: epoxiresin. The recording oscilloscope permitted the input signal to start the ray with an extremely short delay ($1{,}6 \cdot 10^{-7}$ sec), to realize the amplification and time-expansion in calibrated stages, and to store the signal on the oscilloscope screen long enough to be photographed. The sensitivity of this oscilloscope hardly varies between 0 and 10 kcps. The calibration of amplitude and frequency is provided by an internal calibrating unit. Voltage limits: 1 mV/div, resp. 300 mV/div peak to peak; time limits: 10^{-6} s/div, resp. 1 s/div, (LÁNYI–RÁKÓCZY, 1969).

For the explosions, usual seismic hole-shooting with Paxit IV explosive was used. (Paxit IV is a mixture of trinitro-toluol, dinitro-toluol and ammon-saltpeter. Its parameters are similar to Nobel's Explosive No. 704, Ammonal No. 3 and Blasting Abelite).

Partly to attain a better coupling, partly for the elimination of the effect of the low-velocity layer, the sensing sonde was placed, in general, in hole. When investigating the effect of the low-velocity layer, the sonde was placed on the bottom of the mud-pit, on the surface. Shots recorded in a hole are shown in Fig. 11, shots recorded on the surface, in Fig. 1.

Manuscript received 5, 5, 1971.
* Roland Eötvös Geophysical Institute, Budapest.

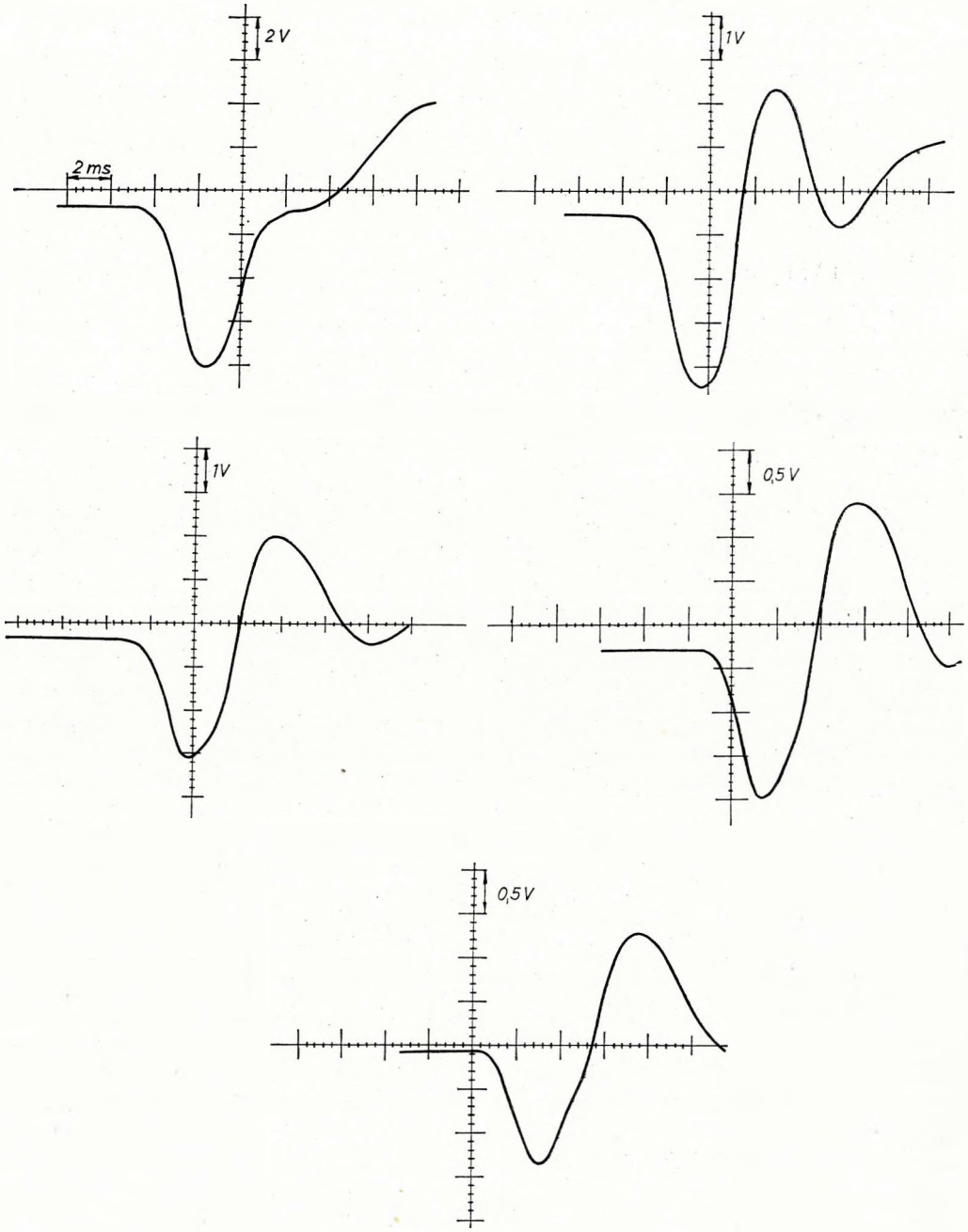

Fig. 1 Series of records observed at increasing source-detector distances (Cf. Table I, Rec. Nos. 5, 4, 3, 2, 1)

1. ábra. Felszínen mért jelsorozat növekvő töltet–szonda-távolság mellett (v. ö. I-es táblázat 5., 4., 3., 2., 1. felvétel)

Рис. 1. Серия сигналов, записанных на дневной поверхности при увеличивающихся расстояниях до пункта возбуждения (см. табл. I. записи 5, 4, 3, 2, 1)

Table I.

List of records

Date	Charge weight, kg	Charge depth, m	Detector depth, m	Charge-detector horizontal distance, (m)	Charge-detector distance, m	Observation	Remark
1. 1969 11 05	1	15	0,3	3,6	15,13	on the surface	
2. 1969 11 05	1	10,5	0,3	3,6	10,82	on the surface	
3. 1969 11 05	1	8,0	0,3	3,6	8,5	on the surface	
4. 1969 11 05	1	5	0,3	3,6	5,92	on the surface	
5. 1969 11 05	1	3	0,3	3,6	4,5	on the surface	
6. 1969 11 05	1	15	0,3	3,1	15,02	on the surface	
7. 1969 11 05	1	9	0,3	3,1	9,24	on the surface	
8. 1969 11 05	1	3,5	0,3	3,1	4,46	on the surface	
9. 1969 11 05	1	12	0,3	2,6	11,99	on the surface	
10. 1969 11 05	1	6	0,3	2,6	6,26	on the surface	
11. 1968 10 10	1	10	10	10	10,0	in hole	ghost
12. 1968 10 10	1	15	10	10	11,18	in hole	ghost
13. 1968 10 10	1	30	10	10	22,36	in hole	ghost
14. 1968 10 10	1	40	10	10	31,62	in hole	ghost
15. 1968 10 10	1	50	10	10	41,23	in bole	ghost
16. 1968 10 10	1	20	0	10	22,36	in hole	ghost
17. 1969 04 24	0,125	15	12	17	17,26	in hole	ghost
18. 1969 04 23	0,25	15	12	16	16,28	in hole	ghost
19. 1969 04 23	0,5	15	12	16	16,28	in hole	ghost
20. 1969 04 23	1	15	12	17	17,26	in hole	ghost
21. 1969 04 24	2	15	12	17	17,26	in hole	ghost
22. 1969 04 24	4	15	12	17	17,26	in hole	ghost
23. 1969 04 24	1	10	0	1	10,05	in hole	ghost

Interpretation of records

Records were sampled manually at equidistant rates $\Delta t = 0{,}0002$ sec, resp. $\Delta t = 0{,}00025$ sec. The computations were performed with a MINSK-2 computer. The beginning of the analysed interval of the pulse was the first onset of the pressure wave and the end of the interval was identical with the end of the first period.

The computer program determined for each pulse:

a) the pulse-shape, reduced to zero average and normalized with respect to the amplification used;

b) the minimum and maximum amplitude (A_{min} and A_{max}), the time interval between them (T_1), the pulse width (T), and the average energy of the pulse (Fig. 2).

The spectrum was computed with the well-known formula of the transfer function of digital filters (Robinson–Treitel, 1964).

23 records were analysed altogether (Table I). In case of ghosts the primary pulse and its ghost were analysed separately as well as the composite wave-form.

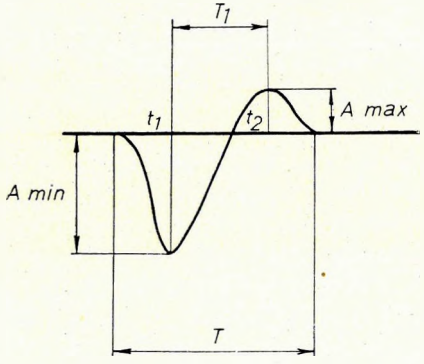

Fig. 2 Characteristics of the primary pulse

2. ábra. A jelalak jellemzői

Рис. 2. Характеристики формы сигналов

Results

The following relations were analysed:

1. the change in pulse shape during propagation;
2. dependence of pulse shape on charge weight;
3. the mechanism of ghost generation.

The results of analysis will be compared with already published theoretical and experimental data, and discrepancies will be tried to be explained. Pulses observed on the surface and those observed in hole will be separately treated, since they show rather different properties, due to the filtering effect of the weathered layer.

Change in pulse shape during propagation

The dependence of amplitude on distance

Pulse amplitudes, when observed on the surface, decreased with increasing shot-detector distance, according to the law

$$A_{min} = \text{const.}\ r^{-1}$$

$$A_{max} = \text{const.}\ r^{-1{,}1}$$

The results apply to a distance interval $r = 4{,}5 - 15$ m and a constant charge weight $W = 1$ kg (Fig. 3.a). The series, recorded in hole, showed a significant, although not regular, decrease.

Dependence of pulse energy on distance

The average energy was found to depend on distance as

$$E = \text{const.}\, r^{-2,32},$$

when measured on the surface. The hole measurements gave

$$E = \text{const.}\, r^{-2,02}, \qquad \text{(Fig. 3.b)}$$

There is a considerable discrepancy among experimental data published on amplitude decrease (Table II). The relatively small exponent found is closest to that observed in water (GRINDA, 1959; LÁNYI–RÁKÓCZY, 1969). This is due to the small range of distances considered. Indeed, the law $E \sim r^{-2,32}$, describing the decrease of energy in the weathered layer, can be written as $E \sim r^{-2} \cdot r^{-0,32}$, where the first factor describes spherical divergence, while the second corresponds to absorption, since, in the range of distances in question, $r^{-0,32} \approx e^{-2\alpha r}$ with $\alpha = 0{,}14\ \text{m}^{-1}$ being the

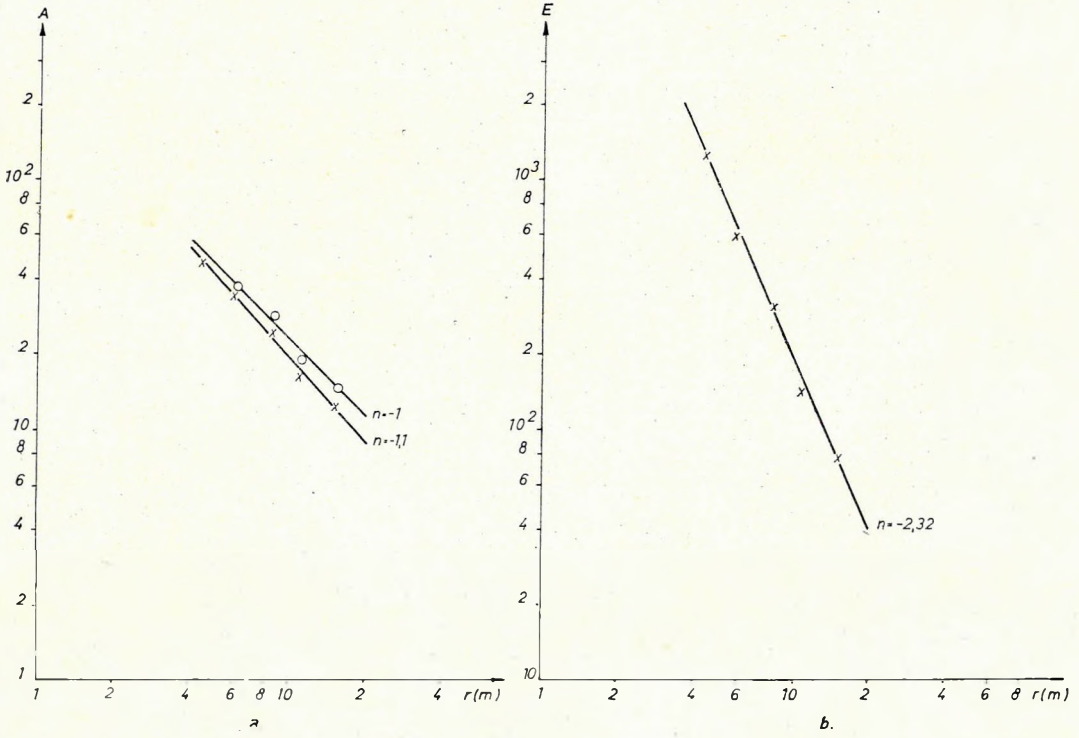

Fig. 3 Amplitude *(a)* and average energy *(b)* values observed on the surface, as functions of distance

3. ábra. Felszínen mért amplitúdó *(a)* ill. átlagenergia *(b)* értékek a távolság függvényében, állandó töltetsúly mellett

Рис. 3. Зависимость амплитуды (*а*) и средней интенсивности (*б*) от расстояния, при равных величинах заряда

Table II.

Dependence of amplitude on distance

Author	Year	Medium	Range of distance, m	Exponent of divergence	Relation
1. Ricker	1953	clay	15 – 488	$-2.5 \pm 3\%$	$A \sim t^n$
2. Jolly	1953	clay	50 – 152	-2.6	$A \sim t^n$
3. Levin–Lynn	1958	—		$-2.26 \div -2.38$	$A \sim t^n$
4. McDonal et al.	1958	—	30 – 150	$-1.98 \div -2.26$	$A \sim t^n$
5. Duvall	1953	sandy clay resp. granite	1.5 – 6.1	$-1.6 \div -2.5$	$A \sim r^n$
6. Grinda	1959	water		-1.13	$A \sim r^n$
7. Fogelson et al.	1959	granite gneiss	0.7 – 32	-1	$A \sim r^n$
8. Kogan	1961	—	r large	-2	$A \sim r^n$
9. Lányi–Rákóczy	1969	water	50 – 880	-0.9727	$A \sim r^n$
10. O'Brien	1969	clay	3 – 80	$-1.01 \div -1.66$	$A \sim r^n$
11. O'Brien	1969	sandstone	3 – 80	$-1.14 \div -1.69$	$A \sim r^n$
		Dependence of energy on distance			
12. Howell–Kaukonen	1954	—		-2.3	$E \sim r^n$
13. Howell, Jr.–Budenstein	1955	—	3.08 – 357	-1.3; -2.6; -3 -4.4, near shot: -6.9	$E \sim r^n$
14. Fogelson et al.	1959	granite gneiss	0.7 – 32	-2	$E \sim r^n$

absorption coefficient for the dominant frequency of the pulse. It is a general experience that for greater distances the exponent increases, owing to energy losses in reflection, absorption and scattering phenomena.

Relation between pulse-width and distance

The pulse width T and the time interval T_1 between amplitude minimum and amplitude maximum increases during propagation according to the laws

$$T = \text{const.}\, r^{0,24}$$

$$T_1 = \text{const.}\, r^{0,35}$$

(detector on surface) and

$$T = \text{const.}\, r^{0,42}$$

$$T = \text{const.}\, r^{0,80}$$

(detector in hole; Fig. 4). The results obtained are in conformity with literary data:

$T = \text{const.}\, t^{0,5}$ (RICKER, 1953),

$T = \text{const.}\, r^{0,37-0,16}$ (O'BRIEN, 1969),

$T = \text{const.}\, t^{0,25}$ (MCDONAL et al., 1958).

Change of the pulse spectrum during propagation

Each pulse was Fourier-analysed between 0–1000 cps. The computed spectra can be considered as reliable between 10–300 cps (below 10 cps the spectrum is distorted by the shortness of records, while above 300 cps it becomes noisy due to reading errors).

It was assumed that the detector's transfer function is not influenced by its orientation and that the initial spectrum of the explosion does not depend on source depth. Fig. 5 shows the spectra of records observed at different source—detector distances. The analysis of these spectra have led to the following conclusions:

From inspecting the spectra of pulses recorded on the surface it is apparent that the total spectral energy decreases with increasing source—detector distance and the dominant frequency shifts toward the lower range during propagation. The decrease of spectral energy can be attributed to the combined effect of spherical divergence and absorption, while frequency shift is due to a frequency-dependent mechanism of the latter. One among the spectra shown in Fig. 5a has a unique shape, it looks like the spectrum of two interfering wavelets. The corresponding record was made above the ground-water table.

Fig. 5b shows spectra of the pulses recorded in hole. The same shift of frequencies can be observed again, the decrease of energy, however, is not so unambiguous, since in these measurements the explosions were performed under slightly different conditions. The spectrum of Rec. No 6 in this series corresponds to an explosion at the same depth but recorded on the surface. It gives, correspondingly, the transfer function of the weathered layer. The weathered layer behaves as a low-pass filter with 90 cps cut-off frequency and 12 dB/octave slope, approximately.

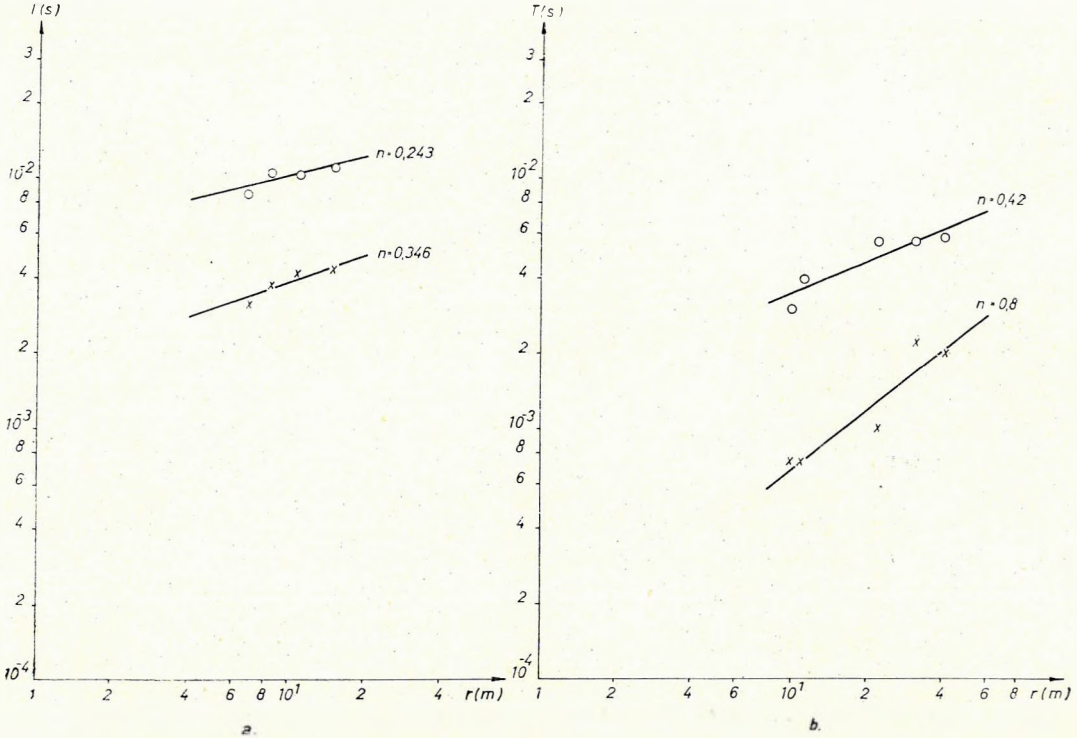

Fig. 4 Pulse width *(e)* and time difference between minimum and maximum amplitudes *(x)*, as functions of distance. Recorded on the surface *(a)*, and in hole *(b)*

4. ábra. Jelszélesség *(e)* illetve maximum—minimum távolság *(x)* a megtett út függvényében *a* — felszínen; *b* — lyukban észlelve

Рис. 4. Зависимость ширины (*e*) и разноса экстремумов сигнала (*x*) от пути пробега, при *a* — наземных; *б* — скважинных наблюдениях

The dominant frequency decreases with increasing source—detector distances, in the order of $r^{-1/3}$ (measured on the surface) and $r^{-2/3}$ (measured in hole). The small deviation from the law describing pulse-broadening is due to the fact that for pulses of not exactly sinusoidal shape, the relation $T = 1/f_{\text{peak}}$ is only approximately valid.

Dependence of absorption on frequency

A frequency-dependent absorption coefficient was determined from the computed spectra of the pulses. We assume that these spectra can be written as

$$Y(\omega) = R(\omega) \cdot S(\omega) \cdot X(r, \omega) \cdot r^{-1} \tag{1}$$

where $R(\omega)$ the source spectrum
$S(\omega)$ amplitude characteristics of the detector
$X(r, \omega)$ attenuation of a harmonic component of angular frequency $\omega = 2\pi f$, after a path of length r.

Let us assume, further, that

$$X(r_1 + r_2; \omega) = X(r_1, \omega) \cdot X(r_2, \omega), \qquad (2)$$
$$X(r, 0) = 1$$

Eq. (2) expresses the homogeneity of the medium and prescribes the usual normalizing constraint. The solution for the functional equation (2) is given by

$$X(r, \omega) = e^{-\alpha(\omega) r}, \quad \alpha(0) = 0,$$

where $\alpha(\omega)$ is some non-negative function of frequency called the (frequency-dependent) absorption coefficient.

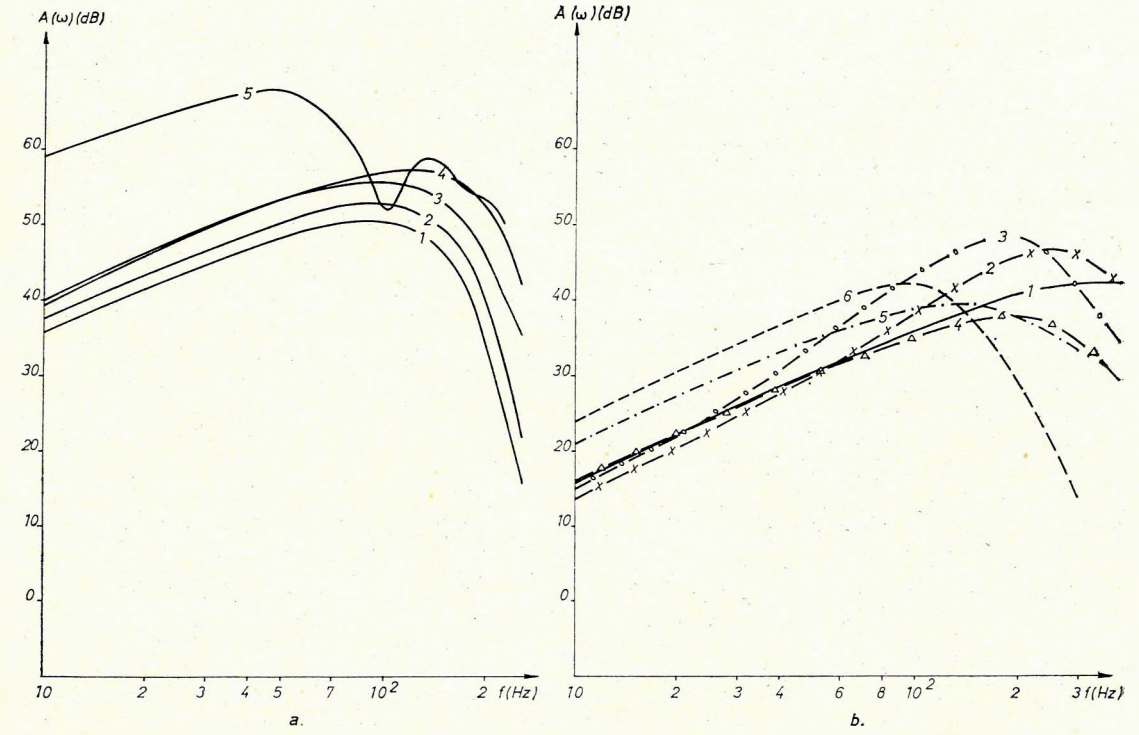

Fig. 5 Amplitude spectra of pulses for different source-detector distances. *a*. Observation on the surface; source-detector distance: *1* 15.13 m, *2* 10.82 m, *3* 8.5 m, *4* 5.92 m, *5* 4.5 m; *b*. Observation in hole; source-detector distance: *1* 10 m, *2* 11.18 m, *3* 22.36 m, *4* 31.62 m, *5* 41.23 m, *6* 22.36 m

5. ábra. Jelek amplitúdó-spekrumai különböző töltet-szonda-távolság esetén, állandó töltetsúly mellett *a)* felszínen észlelve; töltet—szonda-távolság: 1 — 15,13 m; 2 — 10,82 m; 3 — 8,5 m; 4 — 5,92 m; 5 — 4,5 m. *b)* lyukban észlelve; töltet—szonda-távolság: 1 — 10 m; 2 — 11,18 m; 3 — 22,36 m; 4 — 31,62 m; 5 — 41,23 m; 6 — 22,36 m

Рис. 5. Амплитудные спектры сигналов при различных расстояниях до пункта возбуждения и равных величинах заряда

а) наземные наблюдения при расстояниях до пункта возбуждения: *1* — 15,13 м; *2* — 10,82 м; *3* — 8,5 м; *4* — 5,92 м; *5* — 4,5 м;

д) скважинные наблюдения при расстояниях до пункта возбуждения: *1* — 10 м; *2* — 11,18 м; *3* — 22,36 м; *4* — 31,62 м; *5* — 41,23 м; *6* — 22,36 м

Using spectra of pulses recorded at different distances r_1 and r_2 from the source. the detector's transfer function $S(\omega)$ can be eliminated and, assuming that $R(\omega)$ is independent of shot depth, the absorption coefficient can be determined.

In conformity with published theoretical and experimental findings it was found that α obeys the law

$$\alpha(\omega) = \text{const.}\ \omega^n,$$

where, in our case, $n = 2$ for the weathered layer, the attenuation being

$$2{,}3 \cdot 10^{-5} f^2 \text{ dB/m};$$

while measurements performed in hole gave a smaller value $n = 1{,}2$ (Fig. 6). Exponent $n = 1{,}2$ is close to the values usually encountered in literature (Table III), while the f^2 law, describing attenuation in the weathered layer, reproduces Ricker's classic, much debated, result.

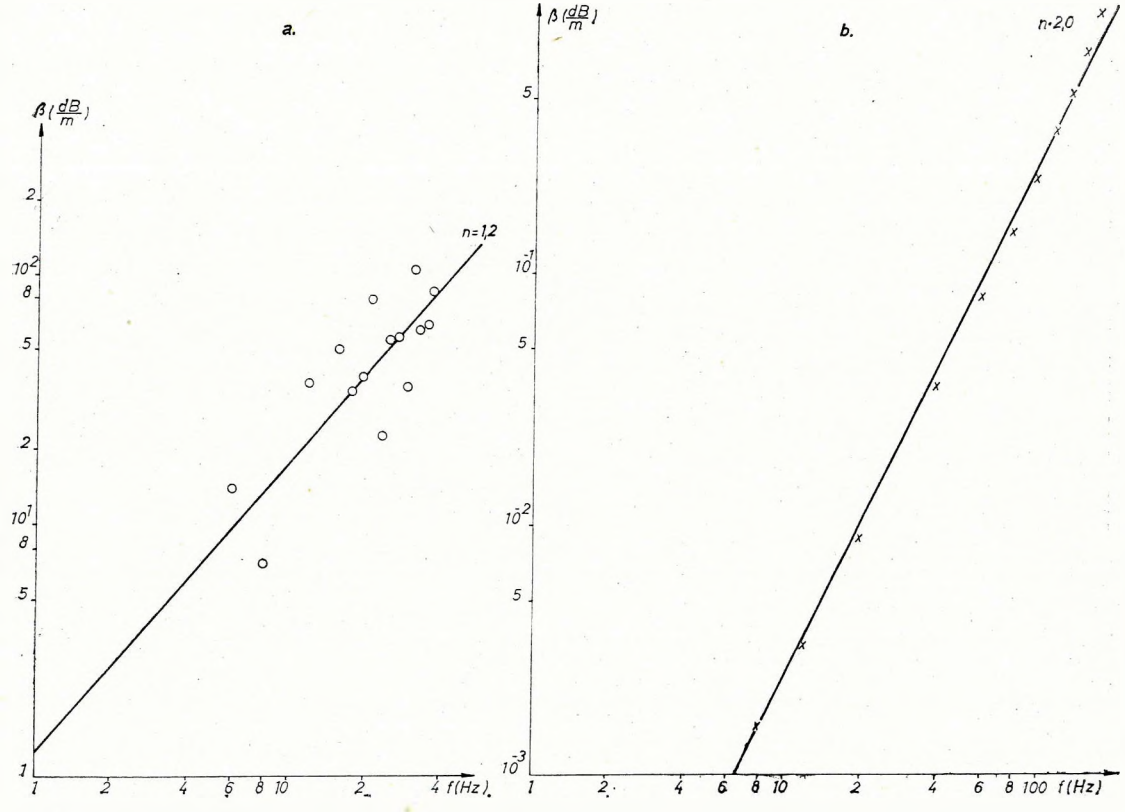

Fig. 6 Coefficient of absorption in function of frequency, *a* in hole, *b* on the surface

6. ábra. Abszorpciós koefficiens a frekvencia függvényében, *a* — lyukban, *b* — felszínen észlelve

Рис. 6. Зависимость коэффициента поглощения от частоты при *а* — скважинных; *д* — наземных наблюдениях

Table III.

Dependence of absorption on frequency

Author	Year	Medium	Range of frequency, cps	Law of absorption
1. Born	1941		22 – 48	$e^{-\delta ft}$; $\delta = 0.023 \div 0.041$
2. Ricker	1953			$e^{-\alpha x}$; $\alpha = \pi f^2/f_0 c$
3. Karusz	1958	sandy clay	80 resp. 200	$e^{-\alpha x}$; $\alpha = 0.19$/m resp. $\alpha = 0.67$/m
4. McDonal et al.	1958		50 – 450	$\alpha = 0.65 f^{1.1}$ dB/1000 ft = $= 2.13 \cdot 10^{-4} f^{1.1}$ dB/m
5. Huang Jen-Hu	1961	clay, sand	20 – 80	$e^{-\alpha x}$; $\alpha = xf^{\beta}$ where: $\beta = 1$; $x = 7.8 \cdot 10^{-5}$/Hzm
6. Attewell–Ramana	1966		$1 - 10^8$	$\alpha = 1.012 \cdot 10^{-5} \cdot f^{0.911}$ dB/cm
7. Mack	1966	sandy clay		$e^{-\frac{\pi \cdot x \cdot f}{Q \cdot c}}$ where $\frac{1}{Q} = 0.012 \pm 0.004$
8. Tullos–Reid	1969			$e^{\alpha f^{\beta} t}$; $\beta = 1 - 1.3$

The dependence of pulse shape on charge weight

In this series of experiments the charge weight varied from 1/8 to 4 kg, the detector was placed in holes at a constant distance $r = 17$ m from the source. The following relations were established:

amplitude vs. charge-weight dependence:

$A_{min} = \text{const.}\ W^{0,54}$;

energy vs. charge-weight dependence:

$E = \text{const.}\ W^{1,07}$.

These relations are illustrated on Fig. 7.

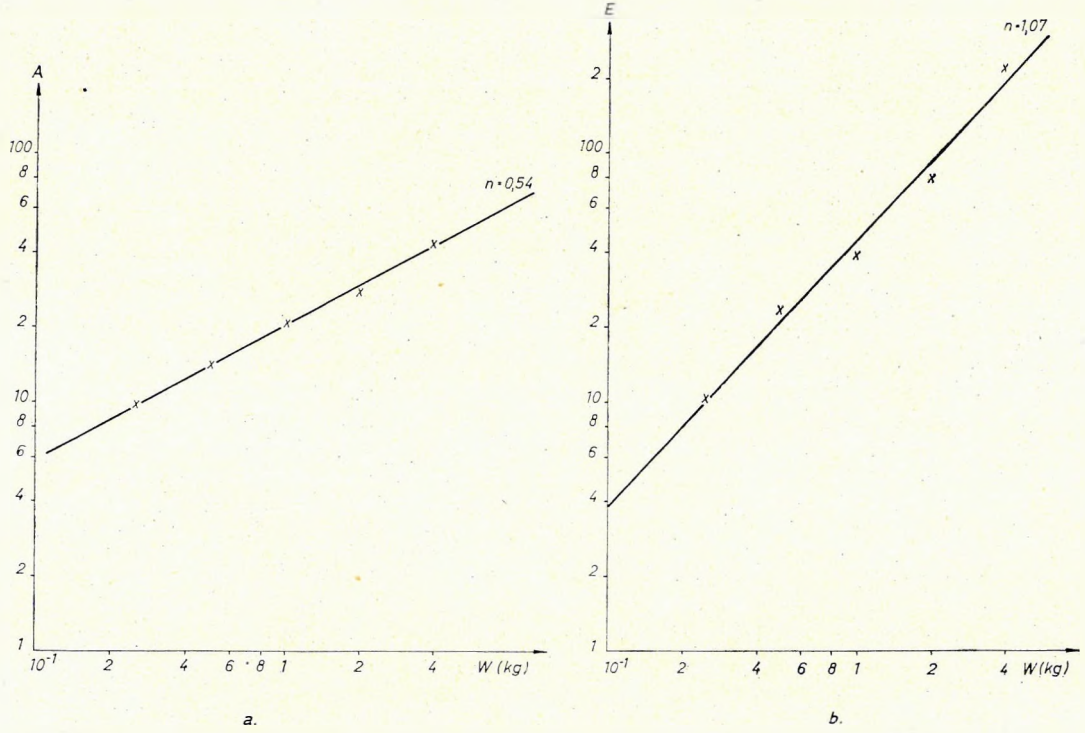

Fig. 7 Amplitude *(a)* and average energy *(b)* values measured in hole, in function of charge weight, for constant source-detector distance

7. ábra. Lyukban mért amplitúdó *(a)* illetve átlagenergia *(b)* értékek a töltetsúly függvényében, állandó töltet—szonda-távolság mellett

Рис. 7. Зависимость величин амплитуд (*а*) и интенсивности (*д*) от величины заряда при постоянных расстояниях зонда до пункта возбуждения, при скважинных наблюдениях

The literature concerning amplitude vs. charge weight relations unanimously accepts the $A = \text{const.} W^n$ law. The exponent n, however, greatly depends on the explosion itself (charge weight, shape and quality of explosive, properties of the surrounding medium, etc.), so a variety of values covering the range $n = 0{,}33 - 1{,}2$ have been reported (Table IV). The exponent found by us is close to that of O'BRIEN, 1969.

Pulse-width vs. charge weight dependence

Pulse width T was found to increase with the 0,13th power of charge weight (see also O'BRIEN, 1969). T_1 showed no significant change (Fig. 8).

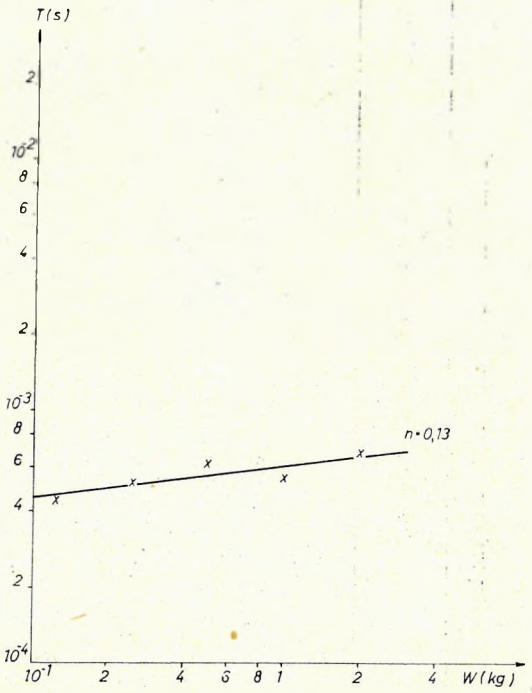

Fig. 8 Pulse width in function of charge-weight

8. ábra. Jelszélesség a töltetsúly függvényében

Рис. 8. Зависимость ширины сигнала от величины заряда

Pulse spectrum vs. charge weight dependence

Fig. 9 illustrates the spectra corresponding to different (1/8–2 kg) charge weights in a constant depth, recorded at a constant distance ($r = 17$ m) from the source. From the analysis of these spectra one may draw the following conclusions:

By increasing the weight of charge the pulse spectrum shifts toward lower frequencies.

Table IV.

Dependence of amplitude on charge weight

Author	Year	Medium	Range of charge weight, kg	Exponent	Remark
1. Barnhard	1967			1/3, 1/2, 2/3, 3/4, 5/6, 1, 7/6	data collected from literature
2. Habberjam–Whetton	1952		2 – 90	0.805	
3. Gaskell	1956	sandstone	9 – 90	1.11	
4. O'Brien	1957		1 – 136	1.12	
5. O'Brien	1960		1 – 200	2/3	
6. Lányi–Rákóczy	1969	water	0.2 – 30	0.3294	
7. O'Brien	1969	clay	0.8 – 9.5	0.336 – 0.55	
8. O'Brien	1969	sandstone	0.8 – 9.5	0.38 – 0.56	

According to PEET's (1960) theory the peak values of the spectra vs. frequency, in case of different charges are located on a hyperbola $A_{peak} = \text{const.} f^{-2}$. We found $A_{peak} = \text{const.} f^{-0,85}$, the smaller exponent can be attributed to the low-pass character of the weathered layer (cf. PEET, 1960, Section IV).

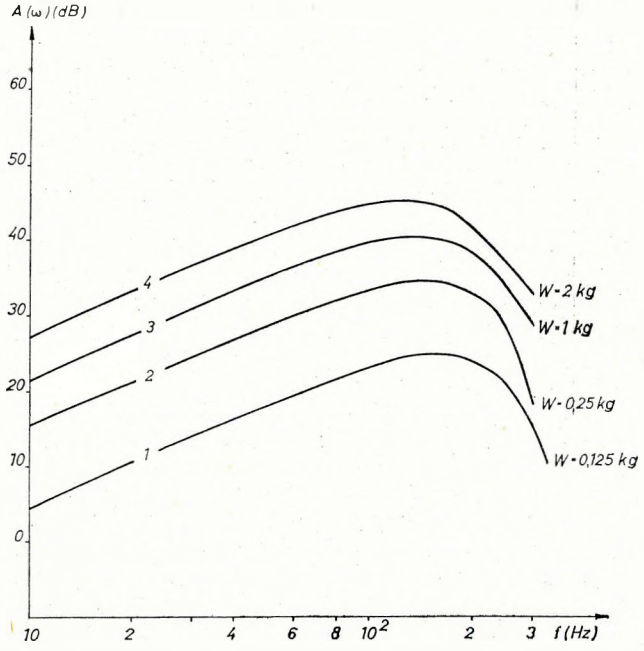

Fig. 9 Amplitude-spectra of pulses for different charge weights (source-detector distance constant)

9. ábra. Jelek amplitúdó-spektrumai különböző töltetsúlyok esetén, állandó töltet—szonda-távolság mellett

Рис. 9. Амплитудные спектры сигналов при разных величинах заряда и равных расстояниях между зондом и зарядом

The dominant frequency was found to depend on charge weight as $f_{peak} = \text{const.} W^{-0,09}$ (Fig. 10). A recent paper of SCHENK (1971) lists experimental and literary data ranging from $n = 0,12$ to $n = 0,28$. It is of interest to note that all experimental values hitherto reported are lower than the theoretical exponent, $n = 1/3$ (PEET, 1960; BLAKE, 1952) which would correspond to the equivalent radiator hypothesis. The spectral amplitude corresponding to dominant frequencies was found to be proportional with $W^{0,5}$. According to PEET (1960) the theoretical exponent is 2/3.

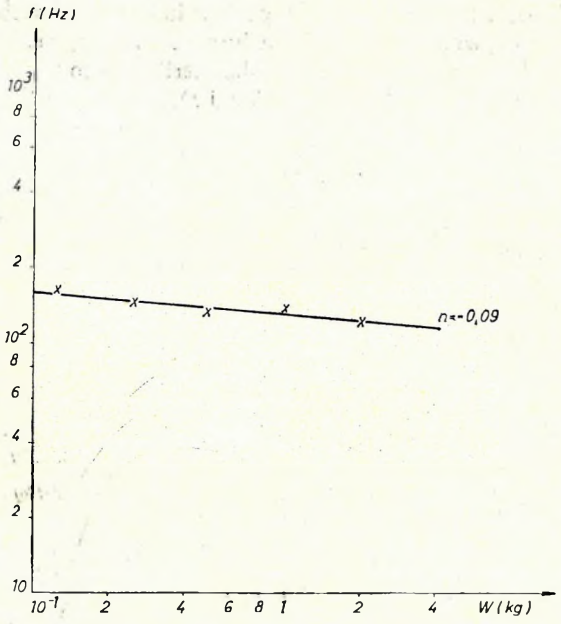

Fig. 10 The dominant frequency in function of charge weight

10. ábra. Csúcsfrekvencia a töltetsúly függvényében

Рис. 10. Зависимость предельных частот от величины заряда

Mechanism of ghost-generation

On certain records (Nos. 11–16, in Table I) the primary pulse was followed by a ghost-arrival. Typical records are shown in Fig. 11.

Figure 12 illustrates the geometry involved in searching for the surface which generates ghosts. From this figure it is obvious that

$$v \cdot t_p = \sqrt{(h_s - h_d)^2 + d^2},$$

$$v \cdot t_g = \sqrt{(h_s - 2h_g + h_d)^2 + d^2},$$

where we have introduced the notations

h_g depth of the ghost-generating surface,

h_d detector depth,

h_s shot depth,

d horizontal source–detector distance,

v average velocity,

t_p, t_g primary and ghost arrival times, respectively.

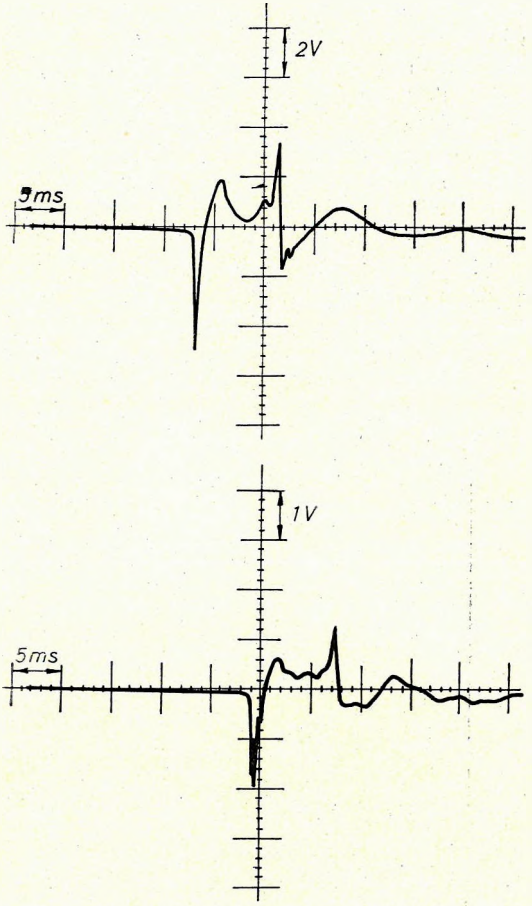

Fig. 11 Typical ghost arrivals
11. ábra. Ghostos felvételek
Рис. 11. Записи с отражениями-спутниками

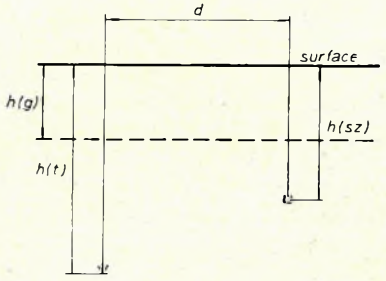

Fig. 12 The geometry of ghost generation
12. ábra. Ghostképződés geometriája
Рис. 12. Геометрия образования отражений-спутников

Using observed values of t_g and t_p, the unknown depth h_g of the surface can be determined. Calculations gave the fair estimation $h_g = 3$–6 m, suggesting that ghost pulses originate from top of the ground-water table. In order to check this hypothesis in another way, we computed the angle of incidence Θ of the ghosts and estimated the corresponding reflection coefficients from the ghost/primary amplitude ratios. The plot of reflection coefficient versus angle of incidence is illustrated in Figure 13. Extrapolating for the case of normal incidence, that is, for $\Theta = 0$, a reflection coefficient $-0{,}45$ is obtained which seems to be realistic for a moist clayey sand—dry sand boundary. Indeed, denoting the acoustic impedances of dry sand and moist clayey sand by Z_1 and Z_2, respectively, we have (cf. GÁLFI et al. 1961, p. 233) $Z_1 \approx 15 \cdot 10^4$ gr cm^{-2} sec^{-1}; $Z_2 \approx 40 \cdot 10^4$ gr cm^{-2} sec^{-1}, and

$$R = \frac{Z_1 - Z_2}{Z_1 + Z_2} = -0{,}45.$$

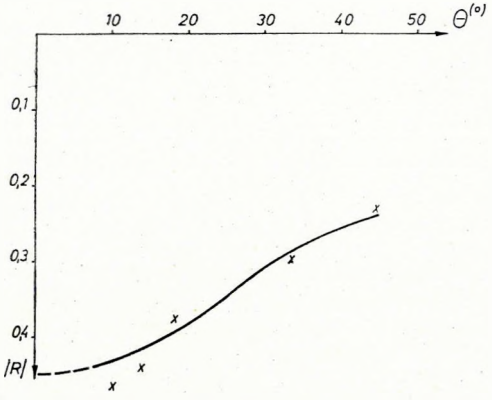

Fig. 13 Dependence of the reflection coefficient on the angle of incidence

13. ábra. Reflexiós együttható a beesési szög függvényében

Рис. 13. Зависимость коэффициента отражения от углов падения

Differences between primary and ghost spectra

As shown in Fig. 14, the spectrum of the composite waveform possesses two isolated peaks indicating that primary and ghost pulses have different spectra. Individual primary and ghost spectra were also determined. The main difference between them is the energy decrease of ghost spectrum, due to spherical and reflection losses and its shift toward lower frequencies, caused by absorption. We have experimental data as yet not enough to elucidate the (presumably frequency-dependent) mechanism of ghost production.

In areas under exploration, measurements of this kind may yield valuable informations for digital processing, since the exact knowledge of ghost/primary amplitude ratio and the time-delay involved is a prerequisite for ghost suppression.

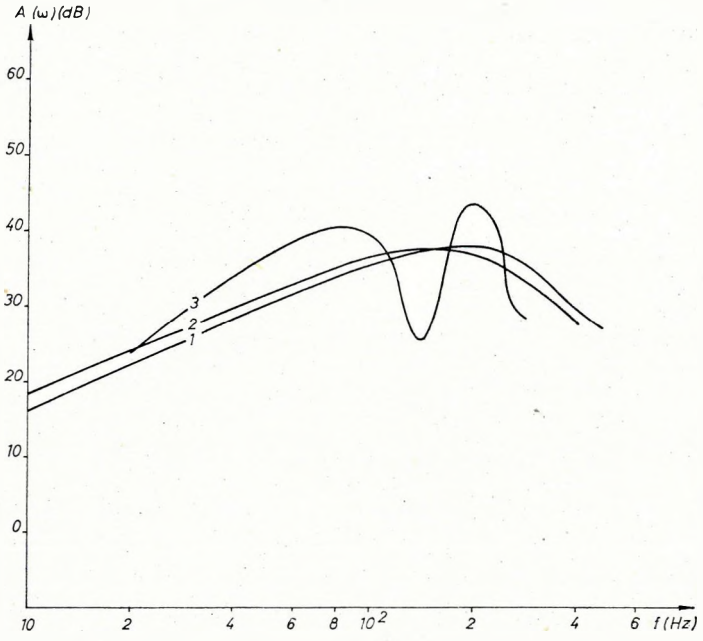

Fig. 14 Amplitude spectra of primary and ghost pulses *1* primary, *2* ghost, *3* combined spectrum

14. ábra. Ghostos felvétel amplitudó-spektruma *1* — jel spektruma, *2* — ghost spektruma, *3* — jel és gost együttes spektruma

Рис. 14. Амплитудный спектр записей с отражениями-спутниками *1* — спектр исгнала *2* — спектр отражения-спутника; *3* — совместный спектр сигнала и отражения-спутника

REFERENCES

Attewell, P. B.–Ramana, Y. V., 1966: Wave attenuation and internal friction as functions of frequency in rocks. Geophysics, XXXI. 6., pp. 1049–1056.

Barnhard, P., 1967: Signal strength of marine explosives. Geophysics, XXXII. 5., pp. 827–832.

Blake, F. G., 1952: Spherical wave propagation in solid media. J. Acoust. Soc. Am. XXIV. 2., pp. 211–215.

Born, W. T., 1941: The attenuation constant of earth materials. Geophysics, VI. 1., pp. 132–148.

Duvall, W. I., 1953: Strain-wave shapes in rock near explosions. Geophysics, XVIII., 2., pp. 310–324.

Fogelson, D. E.–Atchison, T. C.–Duvall, W. I., 1959: Propagation of peak strain and strain energy for explosion-generated strain pulses in rock. Colorado School of Mines Quarterly, LIV. 3., pp. 271–284.

Gálfi, J.–Márton, P.–Meskó, A.–Stegena, L., 1967: Geofizikai Kutatási Módszerek I. Szeizmika. (Methods of Geophysical Exploration I. Seismic methods). Tankönyvkiadó, Budapest.

Gaskell, T. F., 1956: The relation between size of charge and amplitude of refracted wave. Geophysical Prospecting, IV. 2., pp. 185–194.

Grinda, L., 1959: Influence de la profondeur de l'amplitude des ondes sismiques engendrées par une explosion sous-marine. Bolletino di Geofisica, I. 2., pp. 161–174.

Habberjam, G. M.–Whetton, J. T., 1952: On the relationship between seismic amplitude and charge of explosive fired in routine blasting operations. Geophysics, XVII. 1., pp. 116–128.

Howell, B. F. Jr.–Kaukonen, E. K., 1954: Attenuation of seismic wave near an explosion. Bull. Seism. Sec. Am., XLIV., pp. 481–492.

Howell, B. F., Jr.–Budenstein, D., 1955: Energy-distribution in explosion generated seismic pulses. Geophysics, XX. 1., 33–52.

Huang Jen–Hu, 1961: A szeizmikus hullám frekvencia spektrumának kialakulása a gerjesztés, tovaterjedés és észlelés folyamán. Kandidátusi értekezés, Budapest. (Change in the spectral properties of seismic waves during generation, propagation and recording. C. Sc. Thesis, Budapest).

Jolly, R. N., 1953: Deep-hole geophone studies in Garvin County, Oklahoma. Geophysics, XVIII. 3., pp. 662–670.

Карус, Е. В. 1958: Поглощение упругих колебаний в горных породах при стационарном возбуждении. Известия АН СССР, Серия геофизическая, 4, 438—448. (Attenuation of elastic vibrations in solid media)

Коган, С. Я. 1961: Об определении коэффициента поглощения сейсмических волн. Известия АН СССР, Серия геофизическая, 12, 1738—1749. (Determination of the absorbtion coefficient of seismic waves)

Lányi J.–Rákóczy I., 1969: Vízben, robbantással keltett nyomáshullámok terjedésének mérése. Geofizikai Közlemények, XVIII. 3., pp. 97–102. (Investigations of pressure-waves generated by explosion in water).

Levin, F. K.–Lynn, R. D., 1958: Deep hole geophone studies. Geophysics, XXIII. 4., pp. 639–664.

Mack, H., 1966: Attenuation of controlled wave seismograph signals observed in cased boreholes. Geophysics, XXX. 1., pp. 243–252.

McDonal, F. J.–Angona, F. A.–Mills, R. L.–Sengbush, R. L.–Van Nostrand, R. G.–White, J. E., 1958: Attenuation of shear and compressional waves in Pierre Shale. Geophysics, XXIII. 3., pp. 421–439.

O'Brien, P. N. S., 1957: The relationship between seismic amplitude and weight of charge. Geophysical Prospecting, V. 3., pp. 349.

O'Brien, P. N. S., 1960: Seismic energy from explosions. Geophysical Journal, III. pp. 29–44.

O'Brien, P. N. S., 1969: Some experiments concerning the primary seismic pulse. Geophysical Prospecting, XVII. 4., pp. 511–547.

Peet, W. E., 1960: A shock wave theory for the generation of the seismic signal around a spherical shot hole. Geophysical Prospecting, XVII. 4., pp. 509–533.

Ricker, N., 1953: The form and laws of propagation of seismic wavelets. Geophysics XVIII. 1.

Robinson, E. A.–Treitel, S., 1964: Principles of digital filtering. Geophysics, XXIX. 3., pp. 395–404.

Schenk, V., 1971: The predominant frequency of stress waves in non-elastic zone near an explosive source. Geophys. J. R. Astr. Soc. XXII. 4., pp. 347–352.

Tullos, F. N.–Reid, A. C., 1969: Seismic attenuation of Gulf Coast sediments. Geophysics, XXXIV. 4., pp. 516–528.

BODOKY TAMÁS—KORVIN GÁBOR—LIPTAI ISTVÁN—SIPOS JÓZSEF

ROBBANTÁSSAL KELTETT NYOMÁSHULLÁMOK JELLEMZŐINEK VIZSGÁLATA

A dolgozatban ismertetjük az 1968—69-es évben a Nyírségben végzett robbanáshullám kísérletek eredményeit. A méréseket elsősorban az teszi szükségessé, hogy a digitális szeizmikus feldolgozásban, különösen a dekonvolúciós művelet során, elengedhetetlen a jelalak és a jelalak időbeli változásának pontos ismerete. A méréseket homokos összletben végeztük, az észlelést piezoelektromos érzékelővel és Tektronix típusú oszcilloszkóppal hajtottuk végre. A kísérletsorozatban a jelalak változását vizsgáltuk a töltetszonda-távolság és a töltetsúly függvényében. Megállapítottuk, hogy a jelalak amplitúdója r^{-1}; átlagenergiája $r^{-2,3}$; szélessége $r^{0,2-0,4}$; csúcsfrekvenciája $r^{0,3-0,6}$ törvényszerűség szerint függ a távolságtól, a töltetsúly függvényében a jel amplitúdója a $W^{0,5}$, energiája $W^{1,1}$, szélessége $W^{0,13}$, csúcsfrekvenciája $W^{-0,1}$ szerint változik. Az eredmények $W = 1/8 - 4$ kg töltetsúlyokra, és $r = 5 - 50$ m távolságra vonatkoznak. Az eredményeket külön tárgyaljuk lyukban, illetve felszínen végzett észlelés esetére, mert az empirikus kitevők — a laza réteg szűrő hatása miatt — az utóbbi esetben módosulnak. Meghatároztuk az adott közegre jellemző frekvenciafüggő abszorpciós törvényt: felszínközeli összletben a teljes csillapodás $2{,}3 \cdot 10^{-5,2} f^2$ dB/m. Az elsődleges jelet több esetben ghost beérkezés követte (11. ábra). A ghost követési távolságának és amplitúdójának elemzésével bebizonyítottuk, hogy a ghost a talajvízszint határán képződik. Az elsődleges jel és a ghost frekvenciatartalmának eltérése az abszorpció jelenségére utal. A kísérleti eredmények összhangban vannak az irodalmi adatokkal, az esetleges eltéréseket elemezzük.

A dolgozathoz négy táblázat csatlakozik, az első táblázat a mérés körülményeit foglalja össze, a I., III., IV. Táblázatokban összefoglaljuk az amplitúdótávolság függésére, a frekvenciafüggő abszorpcióra és az amplitúdó töltetsúly függésére vonatkozó irodalmi adatokat.

Т. БОДОКИ — Г. КОРВИН — И. ЛИПТАИ — И. ШИПОШ

АНАЛИЗ ХАРАКТЕРНЫХ СВОЙСТВ ПРОДОЛЬНЫХ ВОЛН, ВОЗБУЖДЕННЫХ ВЗРЫВАМИ

В работе описываются результаты опытных работ, проведенных в 1968—1969 гг. в районе Ниршег (Северо-восточная Венгрия) для анализа продольных волн, возбужденных взрывами. Постановка подобного рода исследований была обусловлена тем, что при цифровой обработке сейсмических данных, в частности, при операциях деконволюции, необходимо точно знать формы сигналов и их изменения во времени. Наблюдения проводились в песчаной толще с использованием пьезоэлектрического приемника и осциллоскопа типа Тектроникс. В процессе исследований анализировались изменения формы сигналов в зависимости от расстояния до пункта возбуждения и от величины зарядов. Обнаружено, что для амплитуды сигнала характерна закономерность изменения с расстоянием r^{-1}, для средней его интенсивности — $r^{-2,3}$, для ширины — $r^{0,2-0,4}$ и для предельной частоты — $r^{0,3-0,6}$, а закономерность изменения с величиной заряда выражается для амплитуды — $W^{0,5}$, для интенсивности — $W^{1,1}$, для ширины — $W^{0,13}$ и для предельной частоты — $W^{-0,1}$. Результаты действительны для величин заряда $W = 1/8 - 4$ кг и для расстояний $r = 5 - 50$ м. Раздельно рассматриваются результаты наблюдений, проведенных на дневной поверхности и в скважинах, поскольку эмпирические показатели неодинаковы в связи с фильтрующим эффектом зоны выветривания. Был определен закон изменения поглощения в зависимости от частоты, характерный для данной среды: затухание волн в приповерхностной толще равно $2{,}3 \cdot 10^{-5,2} f^2$ дб/м. За первычным сигналом во многих случаях следовали отражения-спутники (см. рис. 11). Анализ протяженности и амплитуды отражения-спутника позволил сделать вывод о том, что последнее образуется на границе грунтовых вод. Отклонение частотных характеристик первого сигнала и отражения-спутника свидетельствует о наличии поглощения. Полученные результаты согласуются с литературными данными, а причины возможных отклонений анализируются.

К работе прилагаются 4 таблицы, в первой из которых приведены данные об условиях наблюдений, а во второй, третьей и четвертой таблицах представлены литературные данные о зависимостях амплитуды от расстояния, поглощения от частоты и амплитуды от величины заряда, соответственно.